



Contents lists available at ScienceDirect

Opto-Electronics Review

journal homepage: <http://www.journals.elsevier.com/pto-electronics-review>

Light trapping by chemically micro-textured glass for crystalline silicon solar cells

M. Pociask-Bialy^{a,*}, K.D. Mynbaev^b, M. Kaczmarzyk^c^a Department of Experimental Physics, Faculty of Mathematics and Natural Sciences, University of Rzeszow, 1 Pigonia St., 35-959, Rzeszow, Poland^b Department of Laser Photonics and Optoelectronics, School of Photonics, ITMO University, 49 Kronverksky Av., 197101, Saint-Petersburg, Russia^c Department of Building Engineering, Faculty of Civil and Environmental Engineering, Rzeszow University of Technology, 12 Powstancow Warszawy Av., 35-059, Rzeszow, Poland

ARTICLE INFO

Article history:

Received 22 June 2018

Received in revised form 15 October 2018

Accepted 22 October 2018

Available online 10 November 2018

Keywords:

Solar cells

Light trapping

Anti-reflective glass

Texturization

Photoconversion efficiency

ABSTRACT

Results of the studies of optical properties of anti-reflective glasses with various texturization patterns, which were used as a coating for crystalline silicon solar cells, are presented. It was found that glass samples sorted by their optical transmittance demonstrated the same order as when sorted by their solar-cell short-circuit current enhancement parameter. The value of the latter depended on the parameters of texturization, such as the surface density of inclusions and their profile, and the depth of etching pits. A 2% relative increase of the solar cell efficiency was obtained for the best glass sample for null degree angle of incidence, proving enhanced light trapping properties of the studied glass.

© 2018 Association of Polish Electrical Engineers (SEP). Published by Elsevier B.V. All rights reserved.

1. Introduction

Major global producers of photo-voltaic (PV) solar systems strive to reduce production costs and find optimal materials in order to obtain high conversion efficiencies at low prices. So far, the record of the highest efficiency belongs to multi-junction structures (e.g., 46% for four-junction concentrator PV cell [1]), yet the greatest share of the PV market is still possessed by relatively inexpensive silicon solar cells [2]. The record of crystalline silicon (*c*-Si) cell efficiency without a concentrator, 26.6%, was recently set by Kaneka Corporation with the use of heterojunction technology combined with back-contact technology [3]. Important progress in *c*-Si cell efficiency was also achieved thanks to texturization of monocrystalline silicon, a well-known and widely established technique [4]. The efficiency of *c*-Si solar cells can be also improved via application of ultra-thin, nano-patterned films on the surface of the cell [5], and these films may be also used for protecting the cells from harmful environment. However, even the best transparent coatings introduce some opacity that causes a measurable power loss [6,7].

Despite the fact that the start of the development of protective coatings for PV systems dates back to the 50's of the 20th century, these coatings are still being improved and the need for new solutions remains topical. Indeed, photoconversion efficiency of solar radiation by a photosensitive element can be enhanced with the use

of a texturization process [4,8,9], and this process can be applied both to the active cell and to the coating [10,11] (or to the substrate, in the case of the thin-film technology, see, e.g., [12–14]). Typically, the more pronounced the surface morphology changes are, i.e., the stronger the surface roughness, the wider the spectrum of the absorbed solar radiation is [6,7,9]. In this paper, we present the results of the studies of the optical properties of chemically etched glass several samples which were used as a protective coating for *c*-Si solar cells. The measurements of optical transmittance of the glass were related to the results of direct tests of the energy conversion efficiency of the solar cells covered with these glass samples.

2. Samples and methods

The subject of the analysis was eleven samples of the so-called Nano-Selective Transmission-Modelled (NSTM) anti-reflective (AR) glass provided by D.A.Glass Company, Poland. Anti-reflective properties of this glass are achieved not via applying additional surface coatings, but by the chemical treatment of the glass surface (which is very significant from the viewpoint of durability). In particular, one surface of each glass sample possessed chemically embedded micro-inclusions which differed in the surface density and in profiles from sample to sample. The other surface of the glass remained flat and untreated. The details of the treatment procedure are described in details elsewhere [15]. The thickness of glass samples was of ~3.8 mm.

The surface density of the inclusions was determined using the Dino-Lite optical microscope. Glass profiles were measured using

* Corresponding author.

E-mail addresses: pocisk@ur.edu.pl, [\(M. Pociask-Bialy\).](mailto:karim.mynbaev@niuitmo.ru)

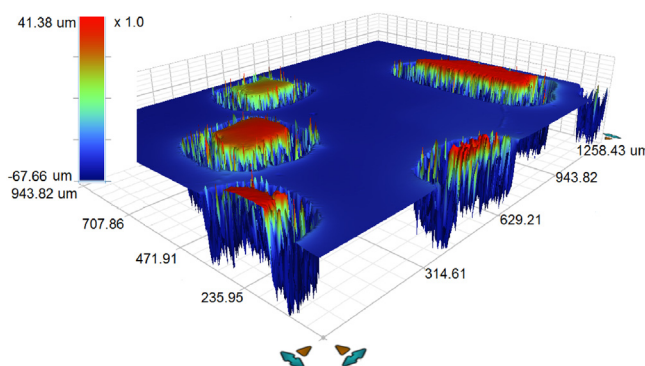


Fig. 1. An example of inclusions in glass sample No. 5. The sizes are in micrometers.

Table 1

Parameters of the studied samples.

Sample No.	Inclusion density, %	Average height of inclusions, μm	Average depth of pits, μm
1	62.1	30.5	49.9
1A	63.0	31.0	49.4
1B	60.2	30.8	51.3
2	59.3	29.5	59.6
3	56.0	32.2	76.7
3A	55.5	32.7	75.4
3B	54	33.2	74.6
4	42.0	26.8	48.0
4A	40	28.7	47.4
4B	43	25.6	49.9
5	28.3	15.0	78.6

ContourGT, Bruker optical profilometer. To determine the density of the inclusions, each sample image was magnified 100 \times and a quarter of 1.5 \times 2 mm surface area was selected for the analysis. The precision of surface area measurement for used magnification equalled 1·10 $^{-3}$ μm^2 . Figure 1 presents an example of the profile of inclusions for one of the samples (sample No. 5, see Table 1). At high magnification, micro-inclusions appear as plateaus surrounded by shallow pits that may resemble moats. Typically, inclusions measured between 100 and 900 μm in length. The parameters of all samples are given in Table 1 (samples with similar parameters were put in one group, like 1, 1A, and 1B, etc.) The surface density of the inclusions was calculated as a ratio of the total surface area of visible inclusions to the total surface area of the studied sample fragment. The process of chemical etching typically affected 60–120 μm of the glass surface.

Modified surface traps electromagnetic radiation via multiple reflections from micro-inclusions which results in a change in scattering properties of the glass. The studied glass is claimed to increase sunlight absorption and to improve parameters of PV cells for high incidence angles, producing a net gain in efficiency of up to 4% for the angles exceeding 60° [16]. In practice, the etched side of the glass that contains the inclusions is typically installed facing the light source (AR configuration). This configuration, however, results in accumulation of dirt in the pits that surround the inclusions. The reversed (F) configuration, when the treated surface faces the cell, makes the cleaning much easier.

3. Results and discussion

Light trapping efficiency, i.e., change in the scattering properties of the glass, was recorded with solar tester certified for silicon PV cell tests, QuickSun130CA, Endes Oy, Finland, AAA + class [17], using pulse xenon lamp as the light source. The trapping was analysed for incident radiation normal to the glass surface. The procedure of determining parameters of solar cells at standard test

conditions (STC) is described elsewhere [18]. What is important is that our set-up allowed for direct testing of the effect of protective coatings on the solar cell operation, thus enabling for the analysis of the optical properties of the coatings [19,20]. Let us note, that previous studies performed in that way [20] dealt only with small, downsized PV modules with the area of several cm 2 . On the contrary, in this study we analysed typical 6" by 6" c-Si solar cells. Also, usually these types of measurements are performed for cells with covers directly laminated on the cell surface during the PV module fabrication process. In our study, we measured optical properties of AR glasses with a 30 mm air gap between the glass and the cell, in accordance with the design of QuickSun130CA tester. On one hand, this introduced energy losses that we had to neglect (and consider the effect of the gap as a systematic error), but on the other hand, this method allows for testing glass properties before the PV module is fully assembled, thus greatly reducing the costs of the tests and, possibly, of the production.

First, the following characteristics of the un-covered solar cell were evaluated with the use of QuickSun130CA: short circuit current I_{SC} , open circuit voltage U_{OC} , maximum power point MPP, fill factor FF, and efficiency η . Next, the cell was partially covered by the studied glass sample, and the current-voltage characteristic of the cell was recorded at STC: power density 1000 W/m 2 , temperature 25 °C, AM 1.5 G. Each measurement was repeated three times, and the averaged values were taken for further consideration. In this way, the measurement accuracies for voltage and current were 0.00002 V and 0.0005 A, respectively. The whole test was conducted twice for all glass samples using two solar cells with different efficiencies. The cells were produced and calibrated at the Fraunhofer Institute, Germany. The value of I_{SC} measured for both cells without any covering served as a reference for further data analysis. The results of the measurements are presented in Table 2.

Relative photo-conversion efficiency values $\eta_{photoconv}$ were calculated for each tested sample in accordance with Bouguer (Lambert) law. Among all registered parameters, I_{SC} , as the most important one, was selected as the basis for the analysis. Value of this parameter is directly proportional to the energy gap, which makes I_{SC} a commonly used parameter for conducting quick quality tests, especially for silicon PV cells. Relative I_{SC} gain ΔI_{SC} [9,11] is described by the following formula:

$$\Delta I_{SC} = \eta_{photoconv}(\text{Textured Sample}) / \eta_{photoconv}(\text{Reference (Non-Textured Sample)}) - 1. \quad (1)$$

Photoconversion efficiency $\eta_{photoconv}$ is given by the equation:

$$\eta_{photoconv} = \text{Real } I_{SC}(\text{Textured Sample}) / \text{Real } I_{SC}(\text{Reference Si cell}), \quad (2)$$

where *Real* I_{SC} (*Reference Si cell*) is the short circuit current recalculated for the reference cell with surface area identical to that of the analysed glass sample. *Real* I_{SC} (*Textured Sample*) is the short circuit current of the cell covered with AR glass reduced by I_{SC} produced by the part of the cell with uncovered surface. As follows from Table 2, each tested AR glass sample was approx. half of the size of the cell used for I_{SC} measurements. To consider this, the signal from the part of the cell that was covered by the glass, was taken as a signal from the entire cell reduced by a signal calculated for the non-covered part of the cell ($\text{Real } I_{SC} = I_{SC} (\text{from the experiment}) - I_{SC} (\text{non-covered cell})$, where $I_{SC} (\text{non-covered cell}) = I_{SC} (\text{reference cell}) (1 - S_{glass} / S_{reference cell})$).

Figures 2, 3 and 4 show how photoconversion efficiency was related to the inclusion density, the height of the inclusions and the depth of the etching pits, respectively. For illustration purposes, the data is given only for one sample in each group. It appears that the best efficiency was achieved for sample 4, which possessed medium values of the inclusion density and the height of inclusions, and

Table 2

Parameters of the cells covered with AR glass with anti-reflective surface facing light source (AR configuration), and facing the cell (F configuration).

Sample	Glass position configuration	$S_{\text{glass}}/S_{\text{cell}}, \%$	c-Si cell No. 1		c-Si cell No. 2	
			I_{sc}, A	Real I_{sc}, A	I_{sc}, A	Real I_{sc}, A
No glass	c-Si	—	8.271	—	8.845	—
1	AR	44.0	7.646	3.014	7.95	2.997
	F	44.0	7.633	3.001	7.948	2.995
1A	AR	44.0	7.702	3.070	7.863	2.910
	F	44.0	7.641	3.009	7.928	2.975
1B	AR	44.0	7.651	3.019	7.952	2.999
	F	44.0	7.465	2.883	8.147	3.1938
2	AR	44.5	7.645	3.057	7.939	3.033
	F	44.5	7.644	3.056	7.945	3.039
3	AR	44.9	7.638	3.0780	7.932	3.058
	F	44.9	7.644	3.086	7.945	3.071
3A	AR	45.0	7.526	2.976	8.047	3.1825
	F	45.0	7.528	2.979	8.049	3.184
3B	AR	45.0	7.526	2.976	8.051	3.186
	F	45.0	7.543	2.994	8.065	3.200
4	AR	45.2	7.659	3.116	7.963	3.116
	F	45.2	7.649	3.126	7.960	3.113
4A	AR	45.2	7.547	3.014	8.083	3.236
	F	45.2	7.550	3.017	8.062	3.215
4B	AR	45.2	7.562	3.029	8.064	3.217
	F	45.2	7.576	3.043	8.049	3.202
5	AR	44.78	7.65	3.083	7.944	3.060
	F	44.78	7.646	3.079	7.947	3.063
6	Without AR	41.54	7.656	2.821	7.975	2.804

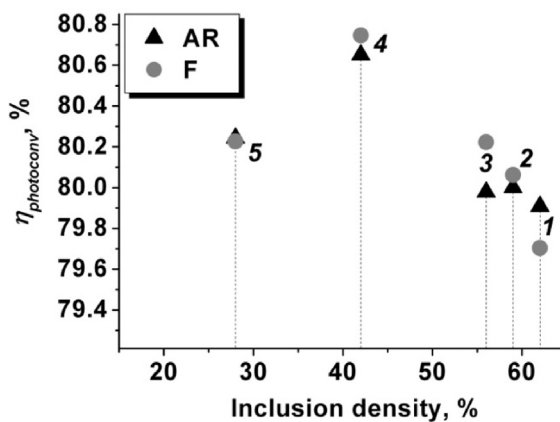


Fig. 2. Photoconversion efficiency vs. the inclusion density for AR and F configurations, shown for samples 1, 2, 3, 4 and 5.

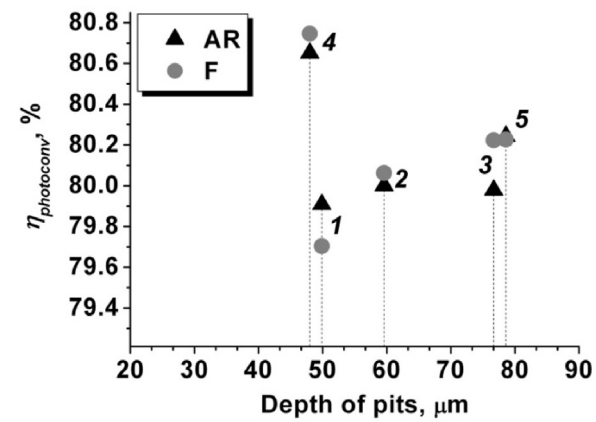


Fig. 4. Photoconversion efficiency vs. the depth of pits for AR and F configurations, shown for samples 1, 2, 3, 4 and 5.

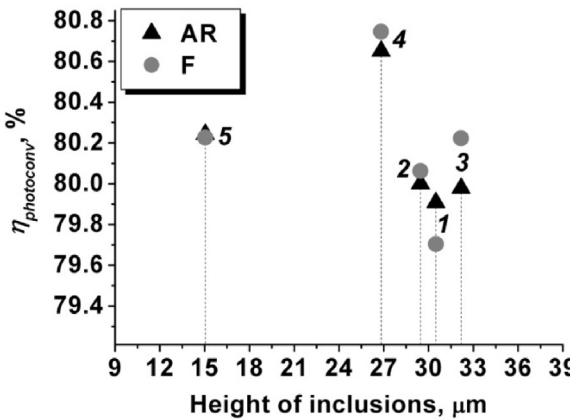


Fig. 3. Photoconversion efficiency vs. the height of inclusions for AR and F configurations, shown for samples 1, 2, 3, 4 and 5.

the shallowest etching pits. The next most effective samples were samples 3 and 5. They had deepest etching pits, but substantially

Table 3

Relative photoconversion efficiencies and relative I_{sc} gains for AR and F configurations.

Sample No.	$\eta_{\text{photoconv.}}, \%$		Relative I_{sc} gain, %	
	AR	F	AR	F
Non-textured	79.211	79.211	—	—
1	79.908	79.703	0.880	0.621
1A	79.813	79.561	0.760	0.442
1B	80.008	79.954	1.006	0.938
2	80.000	80.063	0.996	1.076
3	79.978	80.223	0.968	1.278
3A	79.965	80.018	0.952	1.019
3B	80.021	80.422	1.023	1.529
4	80.650	80.747	1.817	1.939
4A	80.785	80.553	1.981	1.694
4B	80.511	80.749	1.641	1.942
5	80.243	80.226	1.303	1.281

differed in the inclusion density and the height of inclusions. Table 3 summarizes the exact parameters of the efficiency achieved with AR glass samples and compares them to those obtained for c-Si cells covered with the non-textured, plain glass.

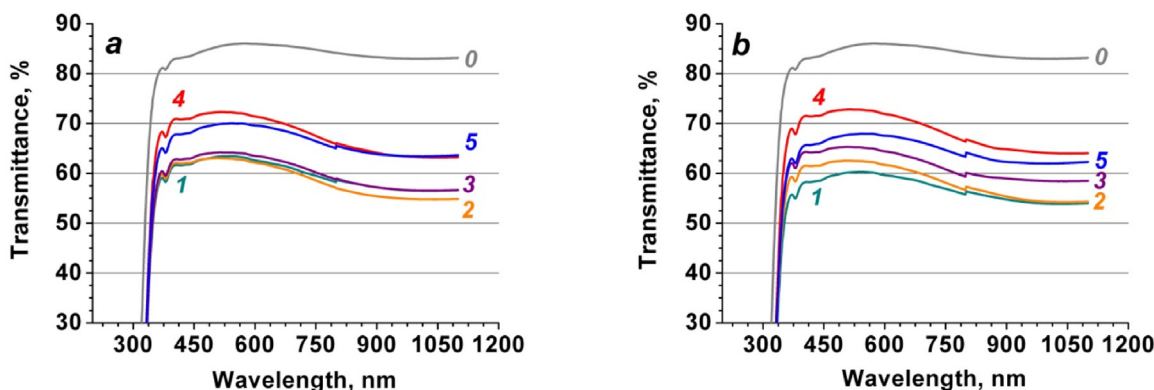


Fig. 5. Transmittance of the non-textured glass sample (curve 0) and that of the treated glass samples 1 to 5 (curves 1–5, respectively) in AR configuration (a) and F configuration (b).

Using an optical spectrometer with integrating sphere manufactured by Instytut Fotonywy, Ltd., we also determined optical transmittance of the samples in the wavelength range of 300 to 1100 nm. Results of these measurements are presented in Fig. 5. Again, for illustration purposes, the data is given only for one sample in each group. It follows from Fig. 5 that, as expected, untreated glass had the highest transmittance in the studied wavelength range. (Here ‘classical’ transmittance, not the scattering properties discussed above is meant. Optical transmittance measurements are performed with a different layout than solar cell tests, using a limited sample area and a photodetector with a small aperture. Thus, though the actual transmittance of untreated glass is higher, the amount of light reaching the solar cell in the tests for this glass may be lower).

The value of the transmittance is typical of 3.2–4 mm-thick low-iron glass, 86% for visible light [7]. The shape of the transmittance spectrum is also typical of that type of glass. In PV system production process, AR configuration is typically used [8,9,11], and this orientation was expected to provide better light trapping for the tested samples, too. In F configuration, the light is first trapped at the “top of the hills” (the reversed pits), and secondly, at the reversed inclusions. This probably resulted in slightly higher transmittances of samples 2, 3 and 4 (Fig. 5b), and a slight increase of the relative I_{SC} gain (Table 3). In this configuration, the transmittance depends on the depth of the pits surrounding the inclusions much more than on the height of inclusions (islands), which is especially noticeable for samples 3 and 4.

Notably, samples of treated glass sorted by their optical transmittance in F configuration demonstrated the same order as when sorted by their short-circuit current enhancement parameter. Thus, the method used allows for performing preliminary tests of glass covers before those are installed in PV systems. Figures 2–4 demonstrate that enhancement of short-circuit current in cells covered by AR glass depended both on the surface density of inclusions and the depth of pits, as well as on the inclusions’ profile. Obviously, in these Figures sample 4 possessed an optimal surface density of inclusions and their profile, as well as relatively favourable depth of the etching pits, which resulted in the most efficient light-trapping. Approximately 2% relative I_{SC} gain (an increase of c-Si cell efficiency) obtained for a cell covered by glass sample 4 proves enhanced light trapping properties of analyzed glass samples for 0° angle of incidence. It is to be expected that further enhancement of light trapping properties may be achieved via reducing the thickness of the glass and subjecting it to additional deepening of the pits. As a result, the protective cover should improve the efficiency of c-Si cells far beyond 4%, which was claimed by the glass manufacturer for the high angles of incidence.

4. Conclusions

In this work, the studies of optical properties of eleven samples of chemically treated low-iron glass differing in texturization pattern (density of inclusions, their profile and depth of etching pits), which were used as a protective coating for crystalline silicon solar cells, were performed. It was discovered that treated glass samples sorted by their measured optical transmittance demonstrated the same order as when sorted by their solar-cell short-circuit current (I_{SC}) enhancement parameter. The value of the latter depended both on the surface density of inclusions and the depth of pits, as well as on the inclusions’ profile. Approximately 2% relative I_{SC} gain (an increase of the cell efficiency) was obtained for a cell covered by glass sample for null degree angle of incidence, proving enhanced light trapping properties of the studied glass.

Author statement

The authors state that their individual contributions to the paper were as following:

M. Pociask-Bialy: conceptualization; data curation; formal analysis; funding acquisition; methodology; project administration; supervision; validation; writing original draft, review and editing.

K.D. Mynbaev: writing original draft, figure formatting and validating, reference acquisition; writing the revised version of the manuscript, review and editing.

M. Kaczmarzyk: data acquisition; data processing; writing original draft.

Acknowledgements

The authors express their thanks for support to European Regional Development Fund and the Polish state budget within the Framework of the Carpathian Regional Operational Programme (RPPK.01.03.00-18-001/10-00) through the funding of the Center for Innovation and Transfer of Natural Science and Engineering Knowledge of the University of Rzeszow.

References

- [1] National Renewable Energy Laboratory (NREL), Golden, CO, United States Department of Energy, Temporal development of best PV cell efficiencies, NREL (2017), <https://commons.m.wikimedia.org> (data presented on May 4, 2017, File: Best Research-Cell Efficiencies.png).
- [2] E. Płaczek-Popko, Top PV market solar cells 2016, Opto-Electron. Rev. 25 (2017) 55–64.
- [3] K. Yoshikawa, H. Kawasaki, W. Yoshida, T. Irie, K. Konishi, K. Nakano, T. Uto, D. Adachi, M. Kanematsu, H. Uzu, K. Yamamoto, Silicon heterojunction solar cell with interdigitated back contacts for a photoconversion efficiency over 26%, Nat. Energy 2 (2017) 17032.

- [4] P. Campbell, M. Green, Light trapping properties of pyramidal textured surfaces, *J. Appl. Phys.* 62 (1987) 243–249.
- [5] M. Stupca, M. Alsalhi, T. Al Saud, A. Almuhan, M.H. Nayfeh, Enhancement of polycrystalline silicon solar cells using ultrathin films of silicon nanoparticle, *Appl. Phys. Lett.* 91 (2007), 063107.
- [6] J.A. Duffie, W.A. Beckman, *Solar Engineering of Thermal Processes*, fourth edition, John Wiley & Sons, Inc., Hoboken, New Jersey, 1980.
- [7] R.B. Wehrspohn, U. Rau, A. Gombert (Eds.), *Photon Management in Solar Cells*, Wiley VCH, Weinheim, 2015.
- [8] S. Tobin, C. Keavney, Experimental comparison of light-trapping structures for silicon solar cells, in: Proceedings of the 20th IEEE Photovoltaic Specialists Conference, 1988, pp. 545–547.
- [9] J. Deubener, G. Helsch, A. Moiseev, H. Bornhöft, Glasses for solar energy conversion systems, *J. Eur. Ceram. Soc.* 29 (2009) 1203–1210.
- [10] J. Müller, B. Rechz, J. Springer, M. Vanecik, TCO and light trapping in silicon thin film solar cells, *Sol. Energy* 77 (2004) 917–930.
- [11] J. Jaus, M. Duell, J. Eckert, F.O. Adurodiya, B. Li, R.A. Mickiewicz, D.M. Doble, Approaches to improving energy yield from PV modules, *Proceedings of SPIE* 7773 (2010) 77730S.
- [12] D. Eisenhauer, H. Sai, T. Matsui, G. Koppel, B. Rech, C. Becker, Honeycomb micro-textures for light trapping in multi-crystalline silicon thin-film solar cells, *Opt. Express* 26 (2018), 315364.
- [13] H. Park, M. Shin, H. Kim, S. Kim, A.H.T. Le, Y. Kim, S. Ahn, J.-S. Jeong, J. Yi, Wideband light scattering of periodic micro textured glass substrates for silicon thin-film solar cells, *J. Nanosci. Nanotechnol.* 17 (2017) 8562–8566.
- [14] W. Zhang, U.W. Paetzold, U. Meier, A. Gordijn, J. Hüpkes, T. Merdzanova, Thin-film silicon solar cells on dry etched textured glass, *Energy Procedia* 44 (2014) 151–159.
- [15] T. Doros, W. Doros, A Method for Manufacturing the Patterned Glass Intended Especially for Building the Solar Collectors and Batteries and Glasshouses, Patent Application WO 2009/104976 A1 (2008).
- [16] DAGlass Company <http://daglass.pl/portfolio/matt-glass/> (Accessed 10 October 2018).
- [17] Endeas Oy Company <http://www.endeas.fi.download/quicksun-800-series/> (Accessed 4 June 2018).
- [18] ASTM E1084-86(2015), Standard Test Method for Solar Transmittance (Terrestrial) of Sheet Materials Using Sunlight, ASTM International, West Conshohocken, PA, 2015, <http://dx.doi.org/10.1520/E1084-86R15> www.astm.org.
- [19] M. Pociask-Bialy, K. Kalwas, Transmittance of selected nanostructurized solar glasses designated via relative change in electrical parameters of silicon solar cells, *EPJ Web Conf.* 133 (2017) 03005.
- [20] M. Ćekon, R. Slávik, P. Juráš, Obtainable method of measuring the solar radiant flux based on silicone photodiode element, *Appl. Mech. Mater.* 824 (2016) 477–484.